Original Research Article

Corrosion Inhibition of Mild Steel in Sulphuric Acid Environment Using Millet Starch and Potassium iodide.

Abstract

Millet starch (MS) was extracted from millet grains and modified using a physical method (pre-gelatinization). The corrosion inhibition effectiveness of millet starch on mild steel corrosion in 0.5 M H_2SO_4 solution was investigated using gravimetric weight loss measurement, potentiodynamic polarization and theoretical chemical quantum computations. The results obtained show that millet starch effectively reduced the corrosion of mild steel in 0.5 M H_2SO_4 solution with an inhibition efficiency of up to 87.14% and 94.03% in combination with potassium iodide. The increase in inhibition on addition of potassium iodide showed synergistic effect. In addition, millet starch was found to function essentially as a mixed-type inhibitor by adsorption on the mild steel surface according to the polarization curves. The mode of inhibition adsorption was best modeled using Langmuir adsorption isotherm. The calculated values of ΔG_{ads}, E_a and ΔH_{ads} suggested physisorption mechanism. Theoretical quantum chemical calculations were performed to confirm the ability of starch to adsorb onto mild steel surface.

Keywords: Millet starch, Langmuir isotherm, adsorption, mild steel, corrosion, Inhibition efficiency

1. INTRODUCTION

Corrosion is one the greatest challenging factors facing the optimal performance of metals and their alloys in aggressive service environment since the inception of industrial revolution, thus subjecting man to several material and financial losses [1]. Corrosion is a non preventable phenomenon (since metals in their purified or refined form are not in their stable state) but can be controlled through the use of inhibitors-an in expensive and effective method for controlling metal corrosion in aqueous aggressive service environments [2]. However, the use of chemical inhibitors such as chromates, nitrates, carbonates, phosphates, molybdates, silicates and other toxic compound as corrosion control inhibitors have proved to be effective inhibitors at relatively low cost but these chemicals create more problems than the solution they offer. Hence, their use should be restricted and penalized due to environmental threat and regulation [3]. The increasing interest in the development of green inhibitors for controlling metal corrosion in unfriendly environment is seen as positive contributions toward safeguarding our challenging environment.

Starch is a natural biodegradable polymer that is renewable, available in abundant at a relatively low cost. It is composed of polysaccharide carbohydrate consisting of a large number of glucose units joined together by glycosidic bonds. The two polymer components of starch are amylose (15 – 20%) and amylopectin (80 – 85%). The amylose and amylopectin ratio in starch determine the functional properties of starch. Starch is extensively used in different applications ranging from food processing, textile, and plastics, paper-making to pharmaceuticals [4]. However, raw starch has limited applications due to some its drawback (such as insolubility in cold water, sensitive to shearing, low pH, etc) but through physical, chemical or enzymatic modification its application range can be enhanced [5]. Several researchers in scientific literature had investigated the use of starch in controlling corrosion of mild steel [1, 6], carbon steel [3, 7-10] and aluminium [11-13] in different aggressive service environment.

The present study does not only experimentally investigate the corrosion inhibition effectiveness of millet starch extracted directly from millet grains, but it also attempts further to obtain in depth mechanistic insights into the corrosion inhibition and adsorption behaviour of millet starch by performing theoretical computations in the framework of the density functional theory (DFT). This approach involves analysis of the molecular electronic structures of the molecule as well as the nature

of the molecule-metal interaction via molecular dynamic simulation. Scanning electron microscopy (SEM) was utilized to give evidence of protection effect of millet starch on the mild surface.

2. MATERIALS AND METHODS

2.1. Sample Preparation

Inhibitor used in the study was pre-gelatinized starch. The starch was extracted from millet grains using the following processes - softening, milling, sieving, decantation, centrifugation and drying described elsewhere. Starch sample obtained was modified by pre-gelatinization (physical or mechanical method) using extrusion technique to obtain starch which is soluble in cold water. Five different concentrations of inhibited solutions ranging from 0.2g/L – 1.4g/L were prepared. H_2SO_4 acid used for the study was BDH grade and 0.5 M H_2SO_4 solution was prepared using serial dilution principle. The potassium iodide (KI) from BDH Laboratories Supplies was used. 0.4gKI was prepared and added to each of the solutions containing inhibitor. The mild steel coupons were used as cut (3 x 3 x 0.1cm) without further polishing but were degreased in absolute ethanol, washed with distilled water, dried in acetone and weighed.

3. EXPERIMENTAL SECTION

3.1 Weight loss measurements

This was performed on the weighed mild steel coupons immersed in 200ml of test solutions contained in a glass beaker and kept at room temperature. The coupons were retrieved at 24 h interval progressively for 7 days. At the end of each stipulation immersion time interval, the coupons were retrieved from the test solutions immersed in 20% NaOH solution containing 200g/L of zinc dust to prevent further corrosion reaction, scrubbed with bristle brush, washed with distilled water, dried and reweighed. The weight loss was calculated as the difference between the final weight at a given time and the initial ht. The values recorded were mean values of triplicate determinations. Thus, the corrosion rate (β) values were determined from the expression stated below.

$$\beta(\mathrm{mm/yr}) = \left(\frac{87600\Delta W}{\rho A t}\right) \quad (1)$$

where, ΔW = weight loss in gram(g), ρ = density of the metal coupons (g/cm^3), A = exposed surface area of the metal coupon(cm^2) and t = time of exposure (in hrs).
The percentage inhibition efficiency, % IE was calculated respectively using the equation [14-15] stated below:

$$\%\,\mathrm{IE} = \left[1 - \left(\frac{\beta_{inh}}{\beta_{blank}}\right)\right] x\ 100 \quad (2)$$

where, β_{inh} and β_{blank} are corrosion rates in the presence and absence of inhibitor respective
The degree of surface coverage (θ) was calculated by using the equation [16] stated below:

$$\theta = \left[1 - \left(\frac{\beta_{inh}}{\beta_{blank}}\right)\right] \quad (3)$$

3.2 Potentiodynamic Polarization Measurements

The polarization measurements were carried out using potentiostat/galvanostat Advanced Electrochemical system, model: PARC- 263 controlled by a computer unit through the electrochemical system software provided by POWER-SUITE. The experiments were carried out in a cylindrical glass electrolytic cell containing test solution with standard three electrodes (working electrode – mild steel, graphite rod - counter electrode (CE), and saturated calomel electrode (SCE) - reference electrode (RE)). The working electrodes were connected to copper wire for electrical contact and embedded in a wax leaving a surface area of 1 cm^2 uncovered. The electrodes were connected to the electrolytic cell through luggin capillary. All measurements were carried out using aerated and unstirred solutions maintained at 30 ±1^{O}C in a potential range of ± 250mV versus corrosion potential using linear sweep technique at a scan rate of 0.333mV/s. Before starting the measurements, the working electrode was allowed to corrode freely for 30 minutes to attain steady state potential which was indicated by a

constant potential. Each test was repeated three times to verify the reproducibility of the system. The inhibition efficiency, % IE was calculated using the following expression:

$$\text{Inhibition efficiency, } \%\,\mathrm{IE} = \left(\frac{I_{corr2} - I_{corr1}}{I_{corr1}}\right) \times 100 \quad (4)$$

where, I_{corr1} and I_{corr2} are the corrosion current densities of mild steel coupon in the presence and absence of inhibitor respectively.

3.3Theoretical Studies

All theoretical computations were performed within the framework of DFT (density functional theory) electronic structure programs – Forcite and DMol^3 as contained in Materials Studio 7.0 software (Accelrys Inc.). The electronic structures of starch and the Fe surface were modelled by means of the DFT electronic structure program DMol^3 using a Mulliken population analysis and Hirshfeld numerical integration procedure [17-19]. Electronic parameters for the simulation include restricted spin polarization using the DNP basis set and the Perdew Wang (PW) local correlation density functional. The simulation of the interaction between a single glucose unit of starch molecules and the Fe surface was performed using Forcite quench molecular dynamics to sample many different low energy configurations and identify the low energy minima [20-21]. Calculations were carried out, using the COMPASS force field and the Smart algorithm. The box was comprised of a Fe slab cleaved along the (110) plane and a vacuum layer of 20 Å height. The geometry of the bottom layer of the slab was constrained to the bulk positions whereas other degrees of freedom were relaxed before optimizing the Fe (110) surface, which was subsequently enlarged into a 10 × 8 supercell. Inhibitor molecules were adsorbed on one side of the slab. The temperature was fixed at 298 K, with an NVE (microcanonical) ensemble, with a time step of 1 fs and simulation time of 5 ps. The system was quenched every 250 steps. Optimized structures of starch molecules and the Fe surface were used for the simulation.

4. RESULTS AND DISCUSSION

4.1. Weight Loss Measurements, Corrosion Rates and Inhibition Efficiency

The dissolution of mild steel coupons in 0.5 M H_2SO_4 in the absence and presence of millet starch was studied using weight loss measurement. Table 1 presents the resultant effect of millet starch in controlling the loss of mild steel immersed in sulphuric acid solution. It is observed that there is material loss in both blank and inhibited solutions with change in immersion time but corrosion damage effect showed more manifestation more in blank solution. In addition, the reduction in material loss by millet starch was dependent on concentration, thus indicating that presence of more starch within the acidic solution improved the resistance of mild steel surface towards dissolution.

The effect of millet starch on the corrosion rate of mild steel coupons in 0.5 M H_2SO_4 acid solution was computed using Eqn (1) and shown in Table 1. The results obtained show that millet starch retarded the corrosion process of mild steel coupons at all concentrations studied. This effect is more pronounced with increasing concentration of starch, suggesting that retardation process is sensitive to the amount of starch present in the aggressive solution. Furthermore, the reduction in the corrosion rate with change in time may be attributed to the stability of corroded products which resist the diffusion of corrosive agents into the mild steel surface

The inhibitive effectiveness of the millet starch in reducing the dissolution of mild steel coupons in 0.5 M H_2SO_4 is shown in Table 1. It is clearly seen that inhibition efficiency increases as concentration of the starch increases reaching a maximum value of 87.14% at a higher concentration (1.4g/L) of the starch studied. This indicates that protective tendency of millet starch is concentration dependent. In addition, it is important to recognize that the suppression of dissolution process is not solely due to reactivity of the millet starch with sulphuric acid but also attributed to the adsorption of the millet starch on the metal surface, which limits the dissolution process by blocking the free corrosion sites and hence reducing the rate of metal dissolution.

Table 1: Calculated values of corrosion rate (mm/yr) and inhibition efficiency (%) for mild steel in 0.5 M H_2SO_4 in the absence and presence of MS and MS+KI from weight loss measurement exposed at room temperature

Systems	Corrosion rate (mm/yr)				Inhibition efficiency (IE %)			
	Days				Days			
	1	3	5	7	1	3	5	7
Blank	41.36	32.18	25.75	20.60	—	—	—	—
0.2g/LMS	15.23	12.82	12.46	11.95	63.18	60.16	51.61	41.99
0.6g/LMS	11.56	9.71	8.91	7.83	72.05	69.83	65.40	61.99
1.0g/LMS	7.35	6.86	5.96	5.53	82.23	78.68	76.85	73.16
1.4g/LMS	5.32	4.86	4.53	4.03	87.14	84.90	82.41	80.44
0.2g/LMS+0.4gKI	12.37	11.00	10.51	9.95	70.09	65.82	59.18	51.70
0.6g/LMS+0.4gKI	6.33	6.03	5.75	5.33	84.70	81.26	77.67	74.13
1.0g/LMS+0.4gKI	3.85	4.15	3.83	3.69	90.69	87.10	85.13	82.09
1.4g/LMS+0.4gKI	2.47	3.30	3.11	3.00	94.03	89.75	87.92	85.44

4.2. Effect of Halide Ion Additive

Table 1 and Figure 1 clearly illustrate that presence of potassium iodide showed remarkable improvement on the inhibition efficiency of millet starch in 0.5 M H_2SO_4 acid solution. This significant improvement could be attributed to the faciliting action of potassium iodide in the formation of organo-metallic (Fe-MS) complex between the functional groups present in the starch molecule and charge on the mild steel surface. Hence, the adsorption of the complex onto metal surface enhances the surface coverage and inhibition efficiency. In addition, Figure 7 revealed the contribution of protonated species in controlling the inhibition process. Hence, it has been reported [22] that organic inhibitor exist as protonated or molecular species in acidic solution and the protonated species adsorb on the cathodic regions of the corroding metal surface and retard hydrogen gas evolution reaction (physical adsorption) whereas the molecular species adsorb on the anodic regions of the corroding metal surface and reduce the anodic dissolution process (chemical adsorption). This result confirmed the active role played by iodide ions in forming ion pair on the metal surface which enhance the surface coverage and inhibition efficiency, and also corroborates the physical adsorption mechanism proposed for the adsorption process of the millet starch.

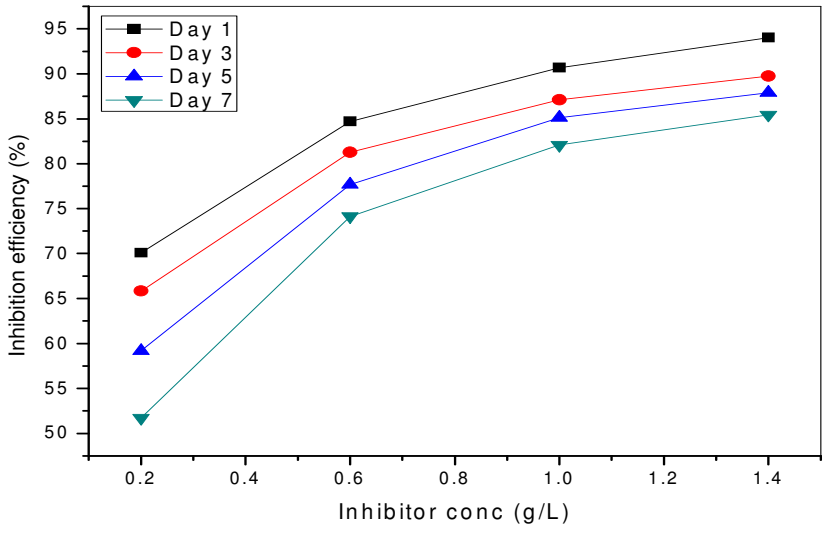

Figure 1: Variation of inhibition efficiency with different concentrations of MS+KI at room temperature

4.3. Adsorption Considerations

In order to characterize the mode of adsorption process of millet starch on dissolution of mild steel in 0.5 M H_2SO_4 acid solution, experimental data from weight loss measurement were fitted to some adsorption isotherms. The adsorption isotherm that best correlates with the experimental data is determined from the closeness of the co-efficient of linear regression (R^2) to unity. Hence, Langmuir adsorption isotherm showed the best fit and was obtained according to the following equations:

$$\text{Langmuir}: \frac{C}{\theta} = \frac{1}{K_{ads}} + C \quad (5)$$

where θ is the surface coverage, K_{ads} is the adsorption-desorption equilibrium constant, C is the inhibitor concentration and g is the adsorbate interaction parameter. Experimental data estimated from weight loss and polarization results were used for plots of C/θ against C presented in parts a and b of Figure 2. Linear plots were obtained with slopes of 1.0653 (R^2 = 0.9920), 1.0005 (R^2 = 0.9994). This is an indication that adsorption of MS and MS+KI on the surface of mild steel followed Langmuir adsorption isotherm, thus supporting the proposed assumptions [23] in derivation of Langmuir adsorption isotherm stated as follows: (a) adsorption sites are uniformly distributed and energetically identical on the metal surface (b) the maximum number of molecules adsorbed is one per adsorption site (c) adsorbate molecules do not interact with each other. The calculated values of K_{ads} from the polarization results in the presence of MS and MS+KI are 8.2102 and 12.7065 respectively. The high value of K_{ads} for MS+KI is evidence that presence of potassium iodide enhanced the adsorption.
The free energy of adsorption (ΔG_{ads}) and equilibrium constant (K_{ads}) in an adsorption-desorption process are related by the expression as follows:

$$\Delta G_{ads} = -RTIn\,(K_{ads}\,x\,55.5) \quad (6)$$

where R is the universal gas constant and T is the absolute temperature. The values of calculated free energy of adsorption were found to be –15.422KJ/mol and –16.522KJ/mol for MS and MS+KI respectively. The negative value of free energy of adsorption is an indication that millet starch is spontaneously adsorbed onto mild steel surface whereas the value of ΔG_{ads} being lower than –20KJ/mol means that millet starch is physically adsorbed onto mild steel surface [24].

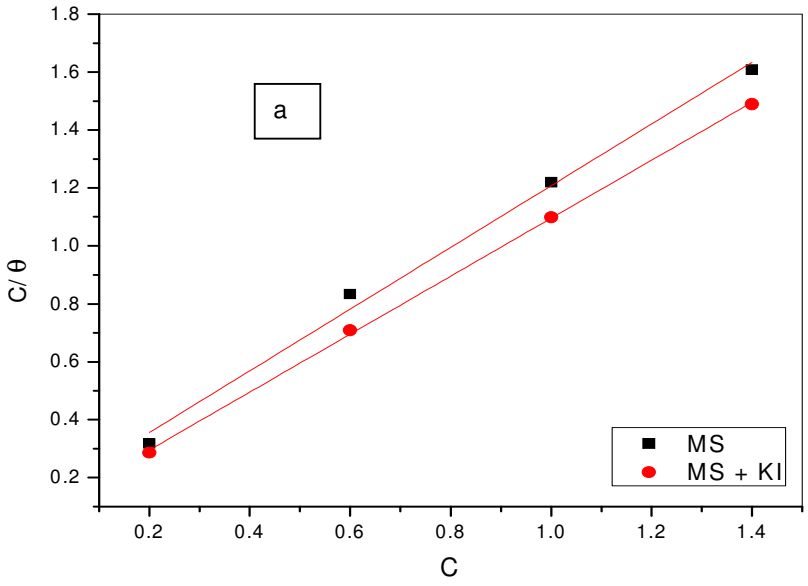

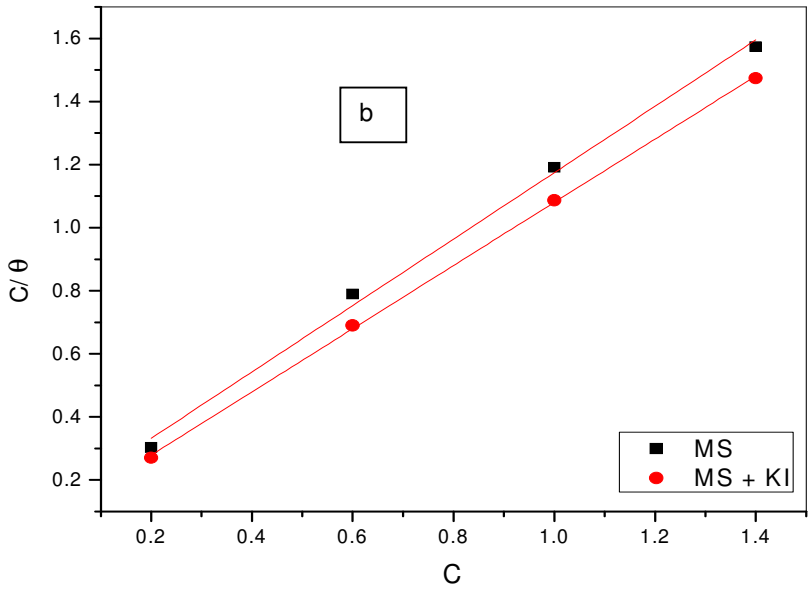

Figure 2: Plots of Langmuir adsorption isotherms (a) weight loss data and (b) polarization data for the adsorption of millet starch on mild steel in 0.5 M H_2SO_4

4.4. Temperature Effect and Thermodynamic Properties

The effect of temperature on the corrosion inhibitive behaviour of MS on mild steel in 0.5 M H_2SO_4 was studied in order to underscore the mechanistic insight of inhibitive performance of millet starch with regards to adsorption and activation processes. For this purpose, the weight loss measurement was employed with the temperature range of $30^{O}C$ – $60^{O}C$ for 4 h immersion. The results obtained are as shown in Table 2. It is observed that the corrosion rate of mild steel in 0.5 M H_2SO_4 solution increase with rise in temperature. However, it is seen that presence of MS and MS+KI in the acidic media decreased the corrosion rate of mild steel, and the trend was concentration dependent. Figure 3 and Table 2 revealed that increase in concentrations of MS and MS+KI enhanced the efficiency of inhibition but as temperature increased the efficiency were reduced, thus suggesting physical adsorption. This could be attributed to desorption of MS and MS+KI adsorbed on the surface of mild steel with increase in temperature and also the corroded product was porous to resist the diffusion of corrosion agents as temperature increased. It has been reported [25] that increase in temperature with reduction in inhibition efficiency suggests physical adsorption mechanism whereas increase in temperature with increase in inhibition efficiency is an indication of chemical adsorption.

Table 2: Calculated values of corrosion rate (mm/yr) and inhibition efficiency (%) for mild steel in 0.5 M H_2SO_4 in the absence and presence of MS and MS+KI starch from weight loss measurement at (30 - 60^{O}C)

Systems	Corrosion rate (mm/yr)				Inhibition efficiency (IE %)			
	30^{O}C	40^{O}C	50^{O}C	60^{O}C	30^{O}C	40^{O}C	50^{O}C	60^{O}C
Blank	81.70	150.98	178.83	224.28	—	—	—	—
0.2g/LMS	32.28	68.10	94.70	171.98	60.49	54.90	47.05	23.32
0.6g/LMS	24.12	48.34	79.66	160.22	70.48	67.98	55.46	28.56
1.0g/LMS	17.05	40.97	58.88	136.35	79.13	72.86	67.07	39.20
1.4g/LMS	13.32	29.47	43.65	119.17	83.70	80.48	75.59	46.87
0.2g/LMS+0.4gKI	29.14	60.25	80.62	152.32	64.33	60.09	54.92	32.08
0.6g/LMS+0.4gKI	20.87	44.77	61.72	130.45	74.46	70.35	65.49	41.84
1.0g/LMS+0.4gKI	13.04	18.81	47.43	103.68	84.04	80.92	73.48	53.77
1.4g/LMS+0.4gKI	8.03	23.52	37.45	83.67	90.17	84.42	79.06	62.69

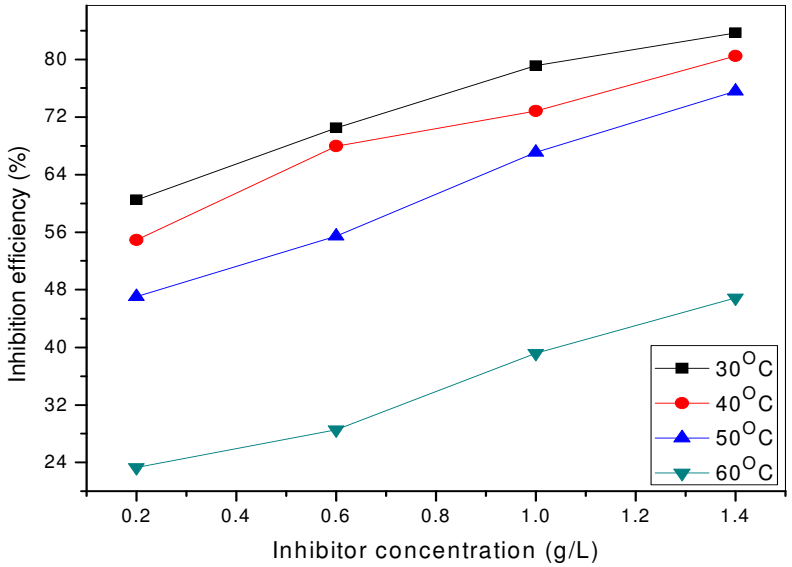

Figure 3: Variation inhibition efficiency versus temperature for mild steel in 0.5 M H_2SO_4 in the presence different concentrations of MS.

The activation energy (E_a) for the corrosion of mild steel in the absence and presence of MS and MS+KI were determined using Arrhenius equation:

$$\log \beta = \log A - \frac{E_a}{2.303RT} \quad (7)$$

where A, E_a, R, T and β represents Arrhenius pre-exponential factor, apparent activation energy, universal gas constant, absolute temperature and corrosion rate. The relationship existing among activation energy, inhibition efficiency and temperature in Eqn (8) is summarized according to Dehri, Ozcan, 2006 [26] as follows: (i) the value of activation energy is greater in inhibited solution than in blank solution for the inhibitors whose inhibition efficiency decreases with rise in temperature. (ii) the value of activation energy is lesser in inhibited solution than in blank solution for the inhibitors whose inhibition efficiency increase with rise in temperature. (iii) the value of activation energy is does not change in both inhibited solution and blank solution for the inhibitors whose inhibition efficiency does not change with variation in temperature. The plots log β against 1/2.303RT for the corrosion process in the absence and presence of MS and MS+KI are shown Figure 4. Linear plots were obtained and values of activation energy (E_a) were determined from the slope and presented in Table 3. High values of activation energy in all cases are compared to values of enthalpy is an indication that gaseous reaction (hydrogen evolution reaction) was involved in the corrosion process and associated with decrease in the reaction volume, thus suggesting physical adsorption mechanism [27-29]. The positive values of enthalpy reflect endothermic process whereas negative and large values of entropy reflect that the activated complex in the rate determining step is an association step, thus indicating that there is a decrease in disorder from reactants to the activated complex [30-32].

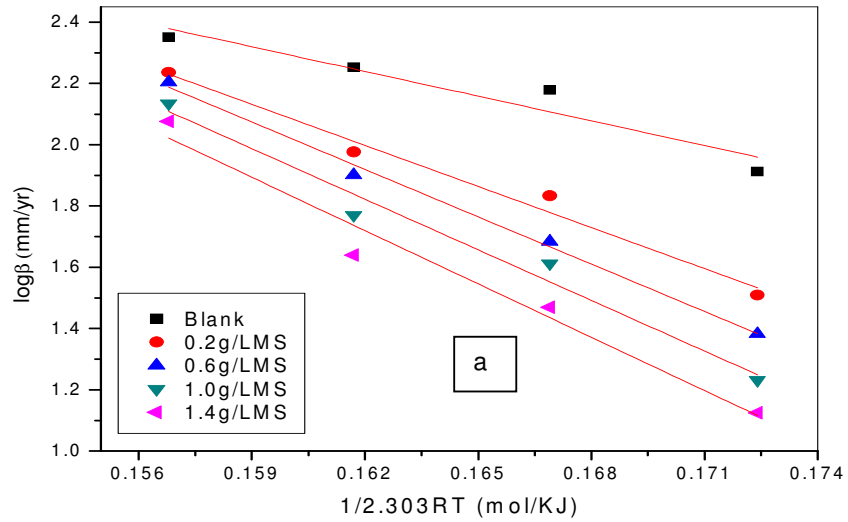

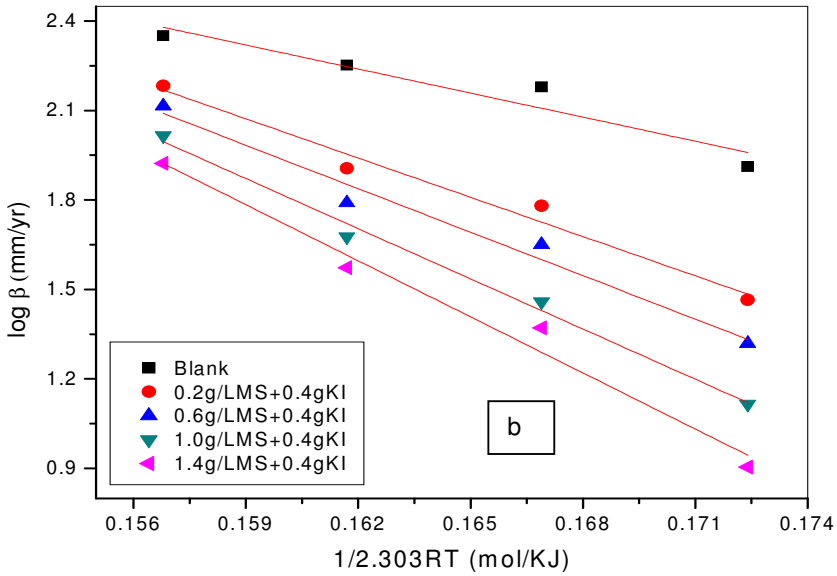

Figure 4: Arrhenius plots of log (β) versus 1/2. 303RT at different concentrations of (a) MS and (b) MS+KI

The enthalpy of activation (ΔH) and the entropy of activation (ΔS) for the corrosion of mild steel in 0.5 M H_2SO_4 were determined by using the Erying transition-state equation:

$$\log\left(\frac{\beta}{T}\right) = \left[\log\left(\frac{R}{hN}\right) + \left(\frac{\Delta S}{2.303RT}\right)\right] - \frac{\Delta H}{2.303RT} \quad (8)$$

where h is the Plank's constant, N is the Avogadro;s number. The plots of log (β/T) versus 1/2.303RT are shown in Figure 5. Linear plots were obtained with slopes equal to 1/2.303R from which ΔH values were obtained whereas intercepts were equal to log [(R/hN + (1/2.303R)] from which ΔS values were determined and presented in Table 3. It was observed that presence of MS and MS+KI in 0.5 M H_2SO_4 acid solution increased the activation energy to values greater than that of blank acid solution, thus suggesting a decrease in the surface available for corrosion due to formation of complex layer (Fe-MS) on the metal surface which altered the corrosion reaction process .

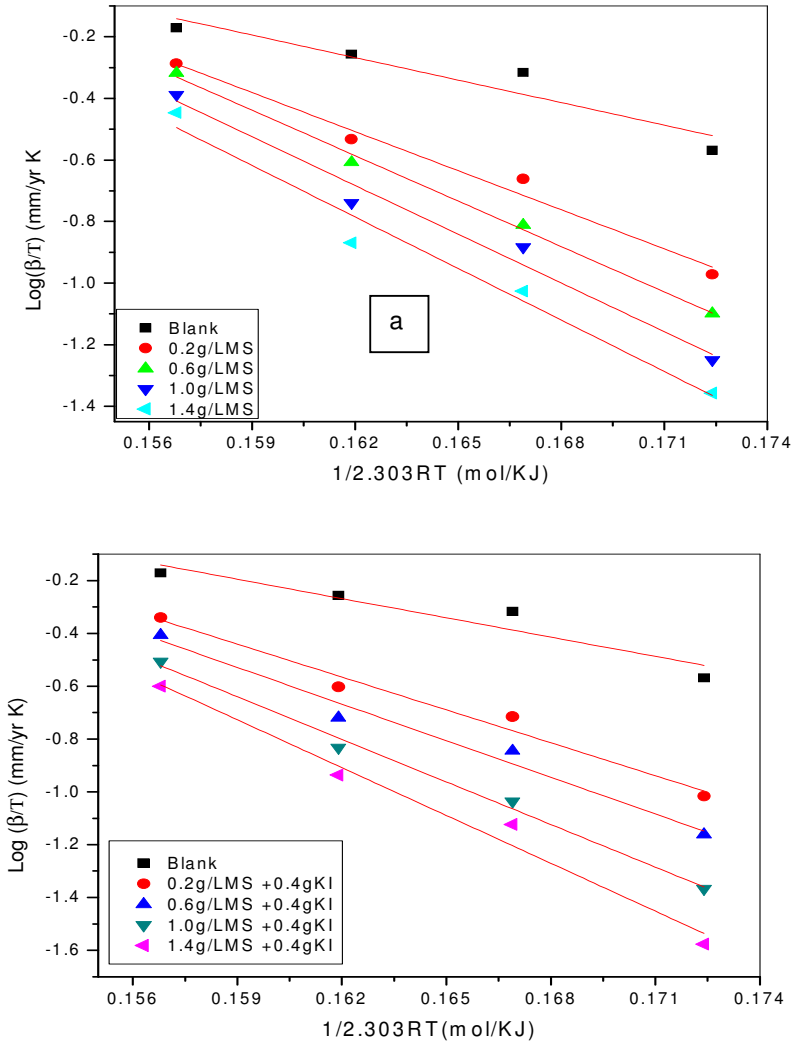

Figure 5: Plots log (β/T) versus 1/2.303RT for mild steel corrosion in 0.5 M H_2SO_4 solution in the absence and presence of (a) MS and (b) MS+KI

Table 3: Calculated values of activation parameters Ea, ΔH and ΔS for mild steel in 0.5 M H_2SO_4 acid solution in the absence and presence of different concentrations of MS and MS+KI.

Systems	Ea (KJ/mol)	ΔH (KJ/mol)	ΔS (KJ/m
Blank	26.886	24.252	–127.506
0.2g/LMS	44.715	42.074	–76.851
0.6g/LMS	51.575	48.953	–57.011
1.0g/LMS	55.106	52.474	–47.952
1.4g/LMS	58.047	55.415	–40.794
0.2g/LMS+0.4gKI	43.885	41.259	–80.468
0.6g/LMS+0.4gKI	48.573	45.947	–67.896
1.0g/LMS+0.4gKI	56.079	53.457	–47.166
1.4g/LMS+0.4gKI	62.700	60.052	–28.764

4.5. Potentiodynamic Polarization Results

The potentiodynamic polarization measurements were used to distinguish the inhibitive effect of millet starch on the hydrogen evolution reaction and mild steel dissolution reaction in 0.5 M H_2SO_4 solution. Figure 6 presents the polarization curves for mild steel corrosion in 0.5 M H_2SO_4 solution in the absence and presence of different concentrations of millet starch. The corrosion current densities (i_{corr}), corrosion potential (E_{corr}), the cathodic (b_c), and anodic (b_a) Tafel slopes estimated from the polarization curves are presented in Table 4. It is observed that rapid dissolution of mild steel occurred in the blank solution and the values of anodic and cathodic current decreased in the presence of MS and MS+KI respectively (for all concentrations studied) when compared to that free acid solution. This is an indication that MS and MS+KI respectively retarded the cathodic hydrogen gas evolution and anodic dissolution of mild steel. The trend of retardation of the partial reactions with the MS and MS+KI respectively is concentration dependent. The corrosion potential E_{corr} of mild steel in the inhibited solutions shifted slightly towards of the negative potential compared to mild steel in the blank solution. Hence, the MS and MS+KI respectively are mixed type inhibitor because the displacement of E_{corr} is less that 85mV [21].

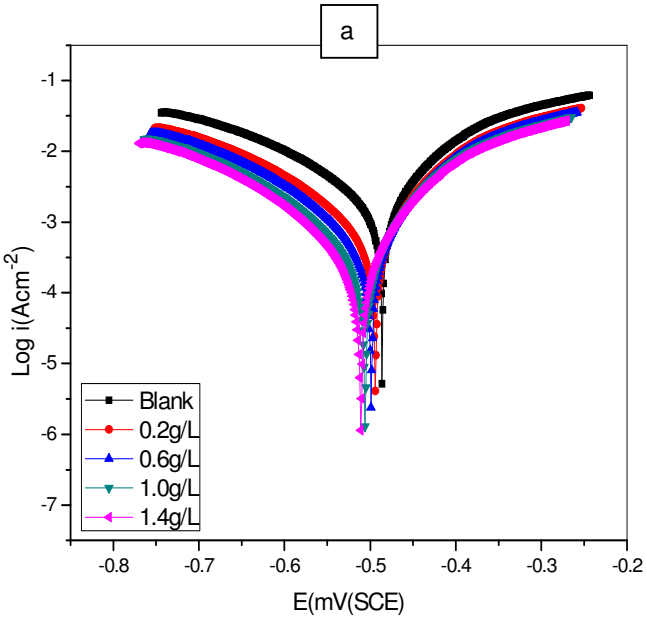

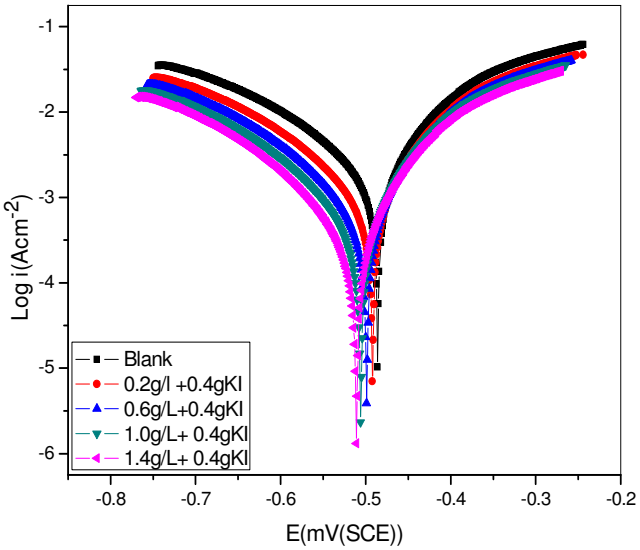

Figure 6: Polarization curves of mild steel in 0.5 M H_2SO_4 in the Absence and presence of (a) MS and (b) MS+KI

Table 4: Polarization parameters for mild steel corrosion in 0.5 M H_2SO_4 in the absence and presence of MS and MS+KI.

Systems	**E_{corr}**	**I_{corr}**	**b_c**	**b_a**	**IE**
	(EmV(SCE))	**(μAcm^{-2})**	**(mVdec^{-1})**	**(mVdec^{-1})**	**(%)**
Blank	–485.83	792.39	183.15	121.76	–
0.2g/LMS	–513.83	267.31	136.43	95.56	66.27
0.6g/LMS	–510.46	193.34	112.68	83.45	75.60
1.0g/LMS	–507.67	123.43	142.87	75.56	84.42
1.4g/LMS	–505.57	83.67	103.32	67.85	88.53
0.2g/LMS+0.4gKI	–503.21	204.25	93.56	57.85	74.22
0.6g/LMS+0.4gKI	–506.24	101.56	106.78	76.78	87.17

1.0g/LMS+0.4gKI	–505.37	62.47	101.56	62.89
92.12				
1.4g/LMS+0.4gKI	–503.64	39.93	97.64	60.45
94.96				

4.7 Theoretical Quantum Computational Studies

Quantum Chemical Studies: Quantum chemical computation is a theoretical framework which provides better insight on the existing relationship the molecular or electronic structure and the corrosion inhibitive effectiveness of an inhibitor. Density functional theory has proved to an important tool in quantum chemical computation due its ability to simulate the geometry optimized molecular structure and as well as predict the descriptors of chemical reactivity of an inhibitor (that is, quantum chemical parameters). Hence, the performance of inhibitors based on their different molecular structures has been linked to their frontier molecular orbital (FMO), including energy of the highest occupied molecular orbital (E_{HOMO}), lowest unoccupied molecular orbital (E_{LUMO}), energy gap between the E_{HOMO} and E_{LUMO} ($\Delta E = E_{LUMO} - E_{HOMO}$). Energy of the highest occupied molecular orbital (E_{HOMO}) measures the susceptibility towards the donation of electron by a molecule, and high values of E_{HOMO} indicate better tendency towards electron donation and inhibition efficiency. E_{LUMO} indicates the tendency of the inhibitor molecule to accept electron usually from the metal atom surface. ΔE is a function of reactivity of the inhibitor molecule towards the adsorption on the mild steel surface. The decrease in ΔE leads to increase in the reactivity of the molecule which increases the inhibition efficiency of the inhibitor. In addition, lower values of ΔE will offer good inhibition efficiency because the energy to remove electron from the last occupied orbital will be low (Obot, Obi-Egbedi, Umoren, 2009; Awad, Mustafa, Abo Elnga, 2010). The geometry optimized structure of glucose molecule, HOMO and LUMO orbitals, Fukui function and the total electron density is presented in Figure 7. The energies of HOMO and LUMO for glucose unit of starch molecule were – 0.5991eV, and – 0.0842eV respectively. The calculated value of ΔE is 0.5149eV. The high value of E_{HOMO} suggests that glucose molecule has the ability to donate electron readily to the mild steel surface whereas the low value of E_{LUMO} indicates tendency to accept electron from the metal atom. The value of ΔE 0.5149eV again reflects the great propensity of the molecule to be adsorbed on the mild steel surface. The adsorption centres on the glucose molecule (that is, local reactivity) was analyzed using Fukui indices to determine the reactive regions in terms of electrophilic and nucleophilic attack. Hence, the region for electrophilic attack is the region where the value of F^- is maximum and it corresponds with the LUMO locations whereas the region for nucleophilic attack is the region where F^+ is maximum and it coincides with the HOMO locations.

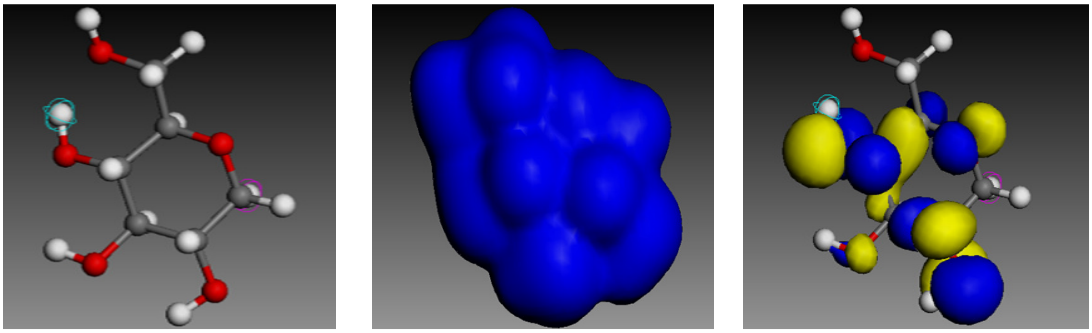

(a) (b) (c)

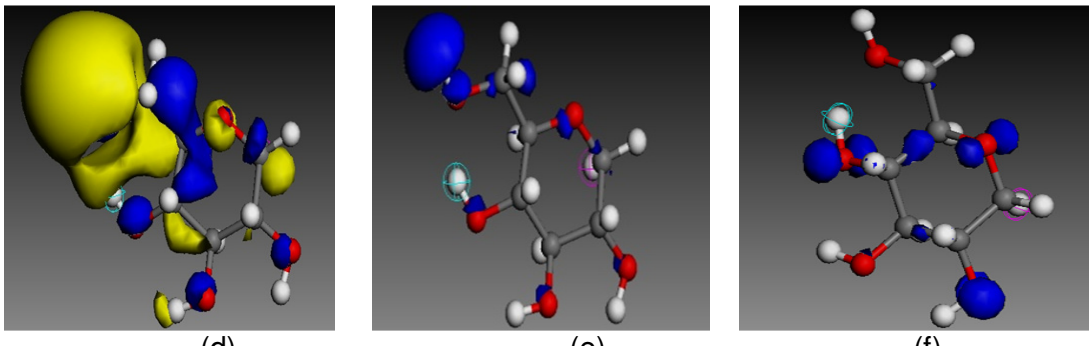

(d) (e) (f)

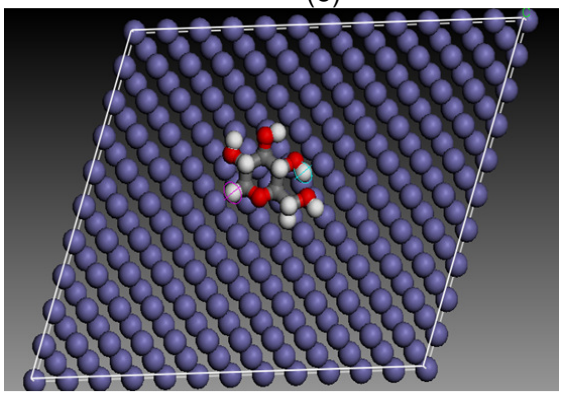

(g)

Figure 7: Electronic properties of glucose unit of starch molecule (a) optimized structure (b) electron density (c) HOMO orbital (d) LUMO orbital, (e) Fukui function for electrophilic attack (F^-), (f) Fukui function for nucleophilic attack (F^+)and (g) top view of the lowest energy adsorption orientation for a single glucose molecule on the Fe (110) surface**.** Atom legend: white = H; gray = C; red = O: The blue and yellow iso-surfaces depict the electron density difference: the blue regions show electron accumulation while the yellow regions show electron loss.

Molecular Dynamic (MD) Simulation: The molecular dynamics (MD) simulations were performed to illustrate the adsorption of the molecules onto the corroding metal surface at a molecular level. This was done using Forcite quench molecular dynamics in the MS Modeling 7.0 software to sample many different low-energy configurations and identify the low energy minima. Calculations were carried out in a 10 x 8 supercell using the COMPASS force field and the Smart algorithm. The Fe crystal was cleaved along the (110) plane. Temperature was fixed at 298 K, with NVE (microcanonical) ensemble, with a time step of 1 fs and simulation time 5 ps. The system was quenched every 250 steps. Optimized structures of glucose molecule and the Fe surface were used for the simulation. Solvent and charge effects have been neglected. The preferred binding sites for the glucose molecules on the Fe surface were obtained from quench molecular dynamics simulation. Figure 7g presents the front view and top view of the lowest energy adsorption orientation for a single glucose molecule on the Fe (110) surface from the simulations. The glucose molecule maintained a flat-lying adsorption orientation on the Fe surface due to delocalization of the electron density all around the molecule. This orientation improves contact with the metal surface and, hence, maximizes the degree of surface coverage.

To determine the adsorption interaction between glucose molecule and the Fe surface, the binding energy ($E_{Binding\ Energy}$) was calculated using the expression shown below:

$$E_{Binding\ Energy} = E_{Total} - (E_{Glucose} + E_{Fe}) \quad (9)$$

where, $E_{Glucose}$ = total energies of the glucose molecule, E_{Fe} = total energies of the Fe (110) slab and E_{Total} = total energies of the glucose and Fe (110) in the gas phase. The total energies of glucose and Fe (110) in the gas phase were calculated by averaging the energies of the five most stable representative adsorption configurations. The calculated binding energy obtained is -82.7518Kcal/mol**.** The negative value of binding energy corresponds to a stable adsorption structure.

However, this is not in full agreement with the strong Starch-Fe interaction as predicted experimentally from the ΔG_{ads} values.

5. CONCLUSION

The inhibitive performance of millet starch towards the corrosion of mild steel in 0.5 M H_2SO_4 solution investigated using the gravimetric weight loss measurement, potentiodynamic polarization and chemical quantum computations established that millet starch was a very good inhibitor, with inhibition efficiency up to 87.14% and 94.03% in combination with potassium iodide. The corrosion inhibition mechanism is based on the adsorption of the glucose unit of starch molecules on the active corrosion sites on the mild steel surface. Polarization measurements suggest that millet starch is a mixed-type inhibitor. The mode of inhibition adsorption was best modeled using Langmuir adsorption isotherm, and the value of the standard free energy of adsorption indicates strong adsorption of the millet starch on the mild steel surface. The trend of inhibition efficiency with temperature variations suggests physical adsorption mechanism. The parameters associated with the electronic structures of millet starch obtained from DFT-based chemical quantum computations confirmed the inhibiting potential of millet starch. This confirmation was further corroborated by molecular dynamic simulations of the adsorption of the single glucose unit from starch molecules onto the mild steel surface. Hence, theoretical results were in agreement with the experimental findings.

REFERENCES

1. Brinda T, Mallika J, Sathyanarayana Moorthy V. Synergistic effect between starch and substituted piperidin-4- one on the corrosion inhibition of mild steel in acidic medium. J. Mater. Environ. Sci, 2015; 6(1): 191-120.
2. Oguzie EE, Wang SG, Li Y, Wang FH. Influence of iron microstructure on corrosion inhibitor performance in acidic media. J.phys.Chem, 2009; 113: 8420-8429.
3. Ochoa N, Bello M, Sancristóbal J, Balsamo V, Albornoz A, Brito JL. Modified cassava starches as potential corrosion inhibitors for sustainable development. Mat. Res, 2013; 16(6): 1209-1219.
4. Omojola MO, Orishadipe AT, Afolaya MO, Adebiyi AB. Preparation and physicochemical characterization of icacina starch citrate - a potential pharmaceutical/industrial starch. Agric. Biol. J.N. Am, 2012; 3(1): 11-16.
5. Akpa JG, Dagde KK. Modification of cassava starch for industrial uses. Inter. Jour. of Egnr and Techn, 2012; 2(6): 913-919.
6. Mobin M, Khan MA, Parveen M. Inhibition of mild steel corrosion in acidic medium using starch and surfactants additives, J. Appl. Polym. Sci, 2011; 121: 1558–1565.
7. Abd El Haleem S, Abd El Rehim S, Shalaby M. Anodic behavior and pitting corrosion of carbon steel in NaOH solution containing chloride ions. Surface and Coating Technology, 1986 27: 167-73.
8. Bello M, Ochoa N, Balsamo V. Effect of the environmental pH on the corrosion bio-inhibitive properties of modified cassava starch. In: proceedings of the 69th Annual Technical Conference and Exhibition. Boston, 2011; 266.
9. Bello M, Ochoa N, Balsamo V, López-Carrasquero F, Coll S, Monsalve A. Modified cassava starches as green corrosion inhibitors of carbon steel: An electrochemical and Morphological approach. Carbohydrate Polymers, 2010; 82: 561-568.
10. Bello M, Sancristóbal J, Ochoa N, Balsamo V. Effect of the degree of substitution of carboxymethylated cassava starch tested as green corrosion inhibitor of carbon steel. ANTEC 2010-Proceedings of the 68th Annual Technical Conference and Exhibition. Orlando. FL, May 16-20. Society of Plastics Engineers, 2010; 115-119.
11. Sugama T, Dubai JE. Polyorganosiloxane-grafted potato starch coatings for protecting aluminum from corrosion. Thin Solid Films, 1996; 289: 39-48.
12. Rosliza R, Wan Nik WB. Improvement of corrosion resistance of AA6061 alloy by tapioca starch in seawater. Current Applied Physics, 2009; 20: 221-29.

13. Kumpawat V, Garg U, Tak RK. Corrosion Inhibition of aluminium in acid media by naturally occurring plant Artocapus heterophyllus and Acacia Senegal, Journ. Ind Council Chem, 2009; 26 (1): 82-4.
14. Prabakaran M, Vadivu K, Ramesh S, Periasamy V. Enhanced corrosion resistance properties of mild steel in neutral aqueous solution by new ternary inhibitor system. J. Mater. Environ. Sci, 2014; 5: 553-564.
15. Obot IB, Ebenso EE, Mwadham Kabanda M. Metronidazole as environmentally safe corrosion inhibitor for mild steel in 0.5 M HCl: Experimental and theoretical investigation. Journ. Environ. Chem Engr, 2013; 1: 431-439.
16. Nwosu FO, Nnanna LA, Okeoma KB. Corrosion inhibition for mild steel in 0.5 M H_2SO_4 solution using achyranthes aspera L. leaf extract, African Journal of Pure and Applied Chemistry, 2013; 7(2): 56-60.
17. Gomez B, Likhanova NV, Dominguez-Aguilar MA, Martinez-Palou R, Vela A, Gazquez JL. Quantum chemical study of the inhibitive properties of 2-pyridyl-azoles. J. Phys. Chem. B, 2006; 110: 8928-8934.
18. Delley BJ. An all-electron numerical method for solving the local density functional for polyatomic molecules. Chem. Phys, 1990; 92: 508–517.
19. Dewar MJS, Zoebisch EG, Healy EF, Stewart JJP. Development and use of quantum mechanical molecular models: A new general purpose quantum mechanical molecular model. J. Am. Chem. Soc, 1985; 107: 3902–3909.
20. Obot IB, Obi-Egbedi NO, Eseola AO (2011). Anticorrosion potential of 2-mesityl-1H-imidazo [4,5-f][1,10]-phenanthroline on mild steel in sulfuric acid solution: Experimental and theoretical study. Ind. Eng. Chem. Res, 2011; 50: 2098–2110.
21. Ferreira ES, Giancomelli C, Giancomelli FC, Spinelli A. Evaluation of the inhibitor effect of L-ascorbic acid on the corrosion of mild steel. Mater. Chem. Phys, 2004; 83: 129–134.
22. Oguzie EE, Enenebeaku CK., Akalezi CO, Okoro SC, Ayuk AA, Ejike EN. Adsorption and corrosion inhibiting effect of Dacryodis edulis extract on low carbon steel corrosion in acidic media. J. Colloid Interface Sci, 2010; 349: 283–292.
23. Nnanna LA, Nwadiuko OC, Ekekwe ND, Ukpabi, CF, Udensi SC, Okeoma KB, Onwuagba BN, Mejeha IM. Adsorption and inhibitive properties of leaf extract of newbouldia leavis as a green inhibitor for aluminium alloy in H_2SO_4, American Journal of Material Science, 2011; 1(2): 143-148.
24. Hussin MH, Kassim MJ. The corrosion inhibition and adsorption behaviour of Uncaria gambir extract on mild steel in 1 M HCl, Mater. Chem and Phys, 2010; 125 (3): 461-468.
25. Oguzie, E.E, Njoku, V.O, Enebeaku, C.K, Akalezi, C.O, Obi, C. Effect of hexamethylparasanline chloride (crystal violet) on mild steel corrosion in acidic media. Corros. Sci, 2008; 50: 3480-3486
26. Dehri I, Ozcan, M. The effect of temperature on the corrosion of mild steel in acidic media in the presence of some sulphur containing compounds. Mater. Chem. Phys, 2006; 98: 316-23.
27. Popova A, Sokolova E, Raicheva S, Christov M. AC and DC study of the temperature effect on mild steel corrosion in acid media in the presence of benzimidazole derivatives, Corrosion Science, 2003; 45(1): 33–58.
28. Oguzie, EE. Influence of halide ions on inhibitive effect of congo red dye on the corrosion of mild steel in sulphuric acid solution, Mater. Chem. Phys. 2004; 87, pp.212-217.
29. Ebenso EE. Effect of Halide ions on the corrosion inhibition of mild steel in H_2SO_4 acid using methyl red. Part 1, Bull Electrochem, 2003; 19: 209-216.
30. Noor EA, Al-Moubaraki AH. Thermodynamic study of metal corrosion and inhibitor adsorption processes in mild steel/1-methyl-4[4'(-X)-styrlpyridium iodides/hydrochloric acid systems. Mater Chem Phys, 2008; 110: 145-154.
31. Toa Z, Zhang S, Li W, Hou B. Corrosion inhibition of mild steel in acidic solution by some oxo-triazole derivatives. Corros Sci, 2009; 51: 2588-2595.

691 32. Badr GE. The role of some thiosemicarbazide derivatives as corrosion inhibitors for C-steel in
692 acidic media. Corros. Sci, 2009; 51: 2529-2536.
693 33. Obot, IB, Obi-Egbedi NO, Umoren, SA. Adsorption characteristics and corrosion inhibitive
694 properties of clotrimazole for aluminium corrosion in hydrochloric acid. Int. J. Electro. Chem.
695 Sci, 2009; 4(6): 863-877.
696 34. Awad MK, Mustafa MS, Abo Elnga MM. Computational simulation of the molecular structure
697 of some triazoles as inhibitors for the corrosion of metal surface. J. Mol. Struc; 2010,
698 THEOCHEM, 2010; 959: 66 - 74.
699 35. Casewit C J, Colwell KS, Rappe AK. Application of universal force field to main group
700 elements. J. Am. Chem. Soc, 1992; 114: 10046–10053.